DAMPING IDENTIFICATION IN BUILDINGS FROM EARTHQUAKE RECORDS

Dionisio Bernal, Salma Mozaffari Kojidi, Kenny Kwan and Michael Döhler

Civil and Environmental Engineering Department, Center for Digital Signal Processing, Northeastern University, Boston, MA

Abstract

Seismic response records from the CSMIP database are used to formulate expressions for the expected value of damping ratios as a function of available regressors. The paper discusses the source of the high variance in the identification of damping and proposes mechanisms for the correlation between fundamental building frequency and damping as well as for the observation that damping increases with the mode number. The data analyzed is restricted to cases where the ground accelerations exceed 0.05g and the values obtained, not surprisingly, prove notably larger than those of previous studies, where very small amplitude vibrations were used. Reduced to the most basic observation the results show that the damping ratio of steel buildings (for linear but not ambient level vibration) is typically larger than the widely used 2%, while 5% is reasonable for concrete.

Introduction

The term damping is used to refer to the collection of mechanisms by which systems dissipate energy. Although the inherent damping of structural systems is not viscous, velocity proportional dissipation is widely used because it leads to mathematical simplicity and because, at least for small damping, it can be calibrated to mimic the actual dissipation well. In practice it is customary to specify damping through modal damping ratios, defined as the quotient of the damping constant of the mode to the minimum value for which the response to arbitrary initial conditions does not have harmonic terms. The problem of extracting damping of viscously damped linear systems from input-output data is a standard problem in identification and exact results are obtained by all consistent algorithms when the data generating system satisfies the assumptions (Juang 1994, Verhaegen and Verdult 2007, Van Overschee and De Moor 1996, Heylen et al. 1997).

Notwithstanding the availability of theory, estimation of consistent damping values from measured response is difficult in structures subjected broadband excitation. The reason for this will be discussed in some detail in the body of the paper but at this point we note that the result is essentially a consequence of the fact that the information (more precisely the Fisher information) encoded in the response data about damping is low. Low information implies that the estimated damping is a random variable with high variance and thus that realizations can differ substantially, either because the data set changes (even though the structure is the same) or because, for a given data set, details of the identification approach vary. One early example of discrepancies in damping estimates obtained for the same data set is that of the 12 high rise buildings subjected to the San Fernando earthquake, considered initially by Hart et al., (1975) and a few years later by McVerry (1979, 1980).

Notwithstanding the high variance, predictors for damping have been derived from the examination of data sets by various researchers. For example, Zhang and Cho (2009) extracted damping ratios from ambient vibration data for 82 buildings in Xi'an, China and proposed an expression for the first mode damping. Other studies include those by Jeary (1986), Lagomarsino (1993), Tamura et al. (1996), Sasaki (1998) and Satake et al. (2003). In most previous studies where large data sets have been considered the vibration amplitudes have been very small and, as a consequence, the damping values obtained can be considered a lower bound. In this study we limited examination to responses where the peak ground acceleration was no less than 0.05g. The cases that satisfied this limit were 69 concrete buildings, 44 steel, 14 masonry and 5 wood structures. Since the response accelerations considered here are significantly larger than in most of the previous studies, we expected the damping values to be larger and the results obtained confirmed this expectation.

In addition to the results of the identification and the regression the paper presents an examination of the variability in damping identification and offers some discussion on the observed trends. The theoretical base of the identification approach is summarized in Appendix A and the numerical values of the identified damping and the regressors for each considered case are presented in Appendix B.

Background and Relations

Equations of Motion

Let the subscript 1 stand for coordinates that are not prescribed and 2 for those that are. The equations of motion of a viscously damped linear system without external excitations can then be written as

$$\begin{bmatrix} M_{11} & M_{12} \\ M_{21} & M_{22} \end{bmatrix} \begin{Bmatrix} \ddot{y}_1 \\ \ddot{y}_2 \end{Bmatrix} + \begin{bmatrix} C_{11} & C_{12} \\ C_{21} & C_{22} \end{bmatrix} \begin{Bmatrix} \dot{y}_1 \\ \dot{y}_2 \end{Bmatrix} + \begin{bmatrix} K_{11} & K_{12} \\ K_{21} & K_{22} \end{bmatrix} \begin{Bmatrix} y_1 \\ y_2 \end{Bmatrix} = \begin{Bmatrix} 0 \\ 0 \end{Bmatrix} \tag{1}$$

The displacements that are not prescribed can be expressed as a linear combination of the prescribed ones plus a residual, namely

$$y_1 = r y_2 + u \tag{2}$$

which, when substituted into the top partition of eq.1 gives

$$M_{11}\ddot{u} + C_{11}\dot{u} + K_{11}u = -(M_{12} + M_{11}r)\ddot{y}_2 - (C_{12} + C_{11}r)\dot{y}_2 - (K_{12} + K_{11}r)y_2 \tag{3}$$

Since the matrix r is arbitrary, it can be selected to cancel any of the terms on the *rhs* of eq.3, taking *r* as

$$r = -K_{11}^{-1}K_{12} \tag{4}$$

neglecting the damping contribution to the *rhs* term, and recognizing that for lumped mass models one has $M_{12} = 0$, one gets

$$M_{11}\ddot{u} + C_{11}\dot{u} + K_{11}u = -M_{11}r\,\ddot{y}_2 \tag{5}$$

which is the conventional expression used to represent earthquake excitation. The point to note here is that the properties on the matrices on the *lhs* of eq.5 are those of the system with restraints at the prescribed coordinates. This means that if only horizontal motion is used to define the input, the properties that a system identification algorithm obtains include the flexibility and dissipation at the soil structure interface in all DOF, other than horizontal translation. For familiarity in the subsequent treatment we drop the subscripts in eq.5 and replace $\ddot{y}_2$ by the more commonly used $\ddot{x}_g$, namely, we use

$$M\ \ddot{u} + C\ \dot{u} + K\ u = -M\ r\ \ddot{x}_g \tag{6}$$

where, for 2D single component input *r* is a vector of ones.

Damping Ratio

Let the *rhs* of eq.6 equal zero, namely

$$M\ddot{u} + C\dot{u} + Ku = 0 \tag{7}$$

the solution to eq.7 is of the form $u(t) = \sum \alpha_i \psi_i e^{s_i t}$ and one finds, by substitution that

$$\left[Ms_i^2 + Cs_i + K \right]\psi_i = 0 \tag{8}$$

where α_i's are scalars. The values of s_i's that satisfy the equation are complex and come in complex conjugate pairs. Writing the solution in terms of its real and its imaginary part, calling on Euler's identity, and replacing *s* by the value at the solution, λ, one finds that

$$u(t) = \sum \alpha_i \psi_i e^{\lambda_{iR} t}(\cos(\lambda_{iI} t) + i\sin(\lambda_{iI} t)) \tag{9}$$

which shows that the rate of decay of the free vibration is determined by the real part of the eigenvalue and the vibration frequency by the imaginary. The definition of damping ratio, which does not require that the damping be classically distributed, is

$$\xi = \frac{-\lambda_R}{|\lambda|} \tag{10}$$

Eq.10 allows for a simple appreciation of why it is difficult to identify damping ratios with low variance. Namely, let the true pole for a given mode be a point in the complex plane and let there be a region around the pole where, due to noise, the identification algorithm places the pole. Assume the region of uncertainty around the pole is a circle of radius *r*, where *r* is a fraction of

the pole magnitude, say $r = \alpha |\lambda|$. Noting that the magnitude of the pole is an estimate of the undamped frequency (exact for classical damping) and recognizing that α is small, one concludes that the variability in frequency is small. The estimation of damping, however, which is given by eq.10, can experience much larger variations. In fact, examination of the geometry shows that the percent error in the frequency is essentially equal to α while the damping ratio, within the uncertainty circle, ranges from the true value to plus or minus α. Let α be 0.02, for example, in this case the frequency error is no more than 2% but the damping ratio can be over or under estimated by 0.02. If the true damping is 5%, one gets values as large as 7% and as low as 3%. To determine if the circular assumption for the uncertainty region is reasonable, we carried out a Monte Carlo study where a system was identified 1000 times using random realizations of the noise. As can be seen from fig.1, which shows results for the first and the second pole, the circular premise is not unreasonable.

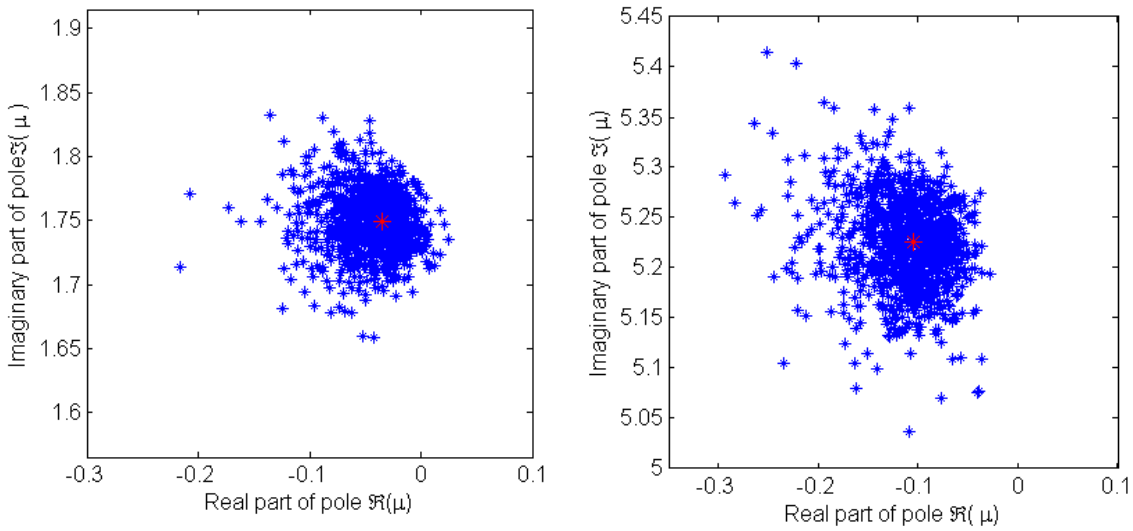

Figure 1. Uncertainty of the real part vs. the imaginary part of the 1st pole and 2nd pole in a 10-DOF system identified using white excitation and 5% additive noise.

Some Proposed Damping Predictors

Predictors for damping in buildings have been proposed through the years and some are summarized next:

Table 1. Damping Predictors

Expression	Source
$\zeta_1 = 0.01 f_1 + 10^{\sqrt{D}/2} x / H$	Jeary (1986)
$\zeta_1 = 0.013 f_1$ (Steel) $\quad \zeta_1 = 0.014 f_1$ (RC)	Satake et al. (2003)
$\zeta_1 = 1.945 + 0.195 T_1^{-3.779}$	Zhang and Cho (2009)
$\zeta_1 = 0.013 f_1 + 0.0029$ (Steel)	Sasaki (1998)
$\zeta_1 = 0.014 f_1 + 470 \frac{x}{H} - 0.0018$ (Steel) $\zeta_1 = 0.013 f_1 + 470 \frac{x}{H} + 0.0029$ (RC)	Satake (2003)
$\zeta_1 = \frac{\alpha}{f_1} + \beta f_1 + \gamma \left(\frac{x}{H} \right)$ $\alpha = 0.0072, \beta = 0.0070$ (RC) $\alpha = 0.0032, \beta = 0.0078$ (Steel)	Lagomarsino (1993)
For higher modes damping ratios: $\zeta_n = (1.3 \sim 1.4) h_{n-1}$ (Steel) $\zeta_n = 1.4 h_{n-1}$ (RC) $\zeta_n = (1.7 \sim 1.8) h_{n-1}$ (SRC)	Satake et al. (2003)

Discussion

Inspection of the expressions in Table 1 shows that the damping ratio tends to increase with frequency and, although only noted in some of the expressions, that it also tends to increase with amplitude. Justification for correlation with amplitude is evident, since some energy dissipating mechanisms "turn on" only when the amplitude crosses some threshold, but the rational for the correlation with frequency is less apparent. We contend here that the causal connection may not be with frequency but with some measure of the size of the interface between the structure and the ground. Another item worth commenting on is the issue of how the damping ratios in higher modes compare to that of the first mode. In this regard Satake (2003) has postulated, based on a trend observed in the first few modes, that the expected value of the damping ratio is higher in the modes above the fundamental. The assertion is consistent with the idea that damping increases with frequency but our contention is that the observation derives from the effectiveness of the mode shape in activating the dissipation mechanism. To illustrate, we formulated a 6-story one bay model where the damping is assumed to come from dashpots of equal magnitude located at each of the connections between beams and columns and computed the equivalent modal damping for the six modes. Results for the case where the behavior is dominated by frame action (relatively rigid beams) and where flexure dominates (relatively flexible beams) are depicted in fig.2. As can be seen, the damping increases in the early modes (magnitude depending on the relative beam-column stiffness) but eventually decreases, as the joint rotations for sufficiently high modes (due to the wavy nature of the mode) are small. It is interesting that the results for the shear type behavior are (in this case at least) in qualitative agreement with the empirical result proposed by Satake for increases from the 1st to 2nd and the 2nd to 3rd mode.

Sensitivity of Identified Damping to Nonlinear Response

While an increase in damping is expected when the amplitude grows, the effect is not as large as one may anticipate. Support for the contention is found in the short duration over which the nonlinearity is activated for earthquake input. To illustrate, the identified frequencies and equivalent damping of a SDOF with a frequency of 1 Hz and 5% viscous damping were obtained from identification for three different response levels using the Whittier ground motion. The first level is linear and is used to confirm that the ID is able to identify the correct model. The other two correspond to nominal displacement ductility levels of 2 and 4. The identified damping values are {5, 5.82, and 8.4} percent and the identified frequencies are {1, 0.99, and 0.98} hertz respectively. The increase in damping, especially at ductility 2 is very modest. Plots of the resulting force vs. drift are depicted in fig.3.

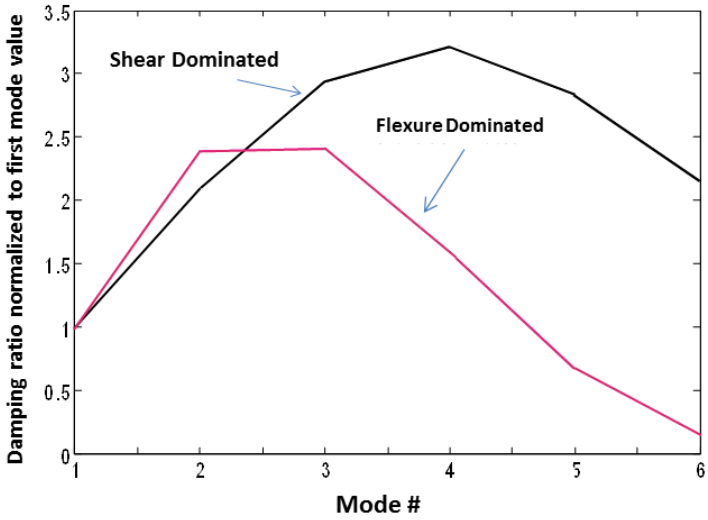

Figure 2. Ratio of damping between various modes in a 6-story model with dissipation simulated with dashpots at the beam-column joints.

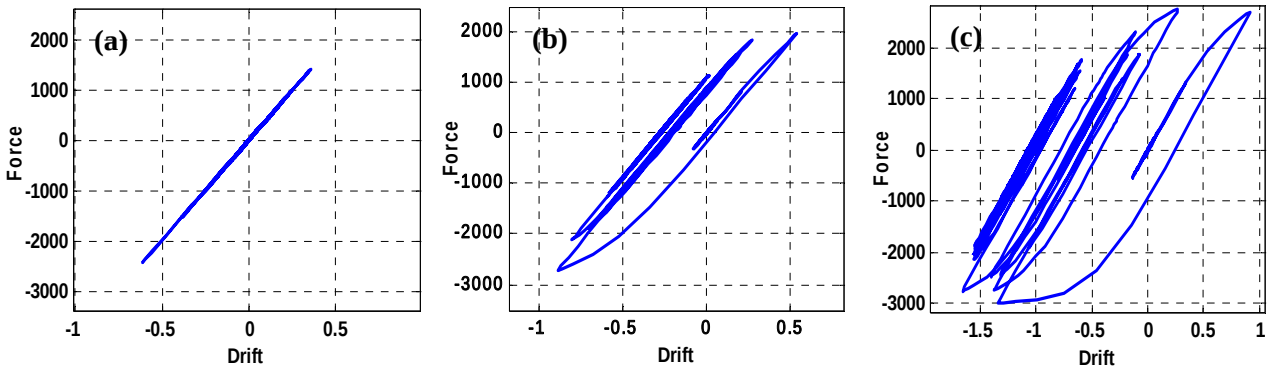

Figure 3. Force vs. drift for three response levels (a)-(c)

Uncertainty in Damping Estimation

This section presents some discussion on the estimation of damping from the perspective of the "information content" of a parameter in available data. It is shown that for conditions that are typical the coefficient of variation of damping ratios can be more than 50 times higher than that of frequencies. Similar results on the identification of ARMA models have been reported in Gersch (1974).

The Cramér-Rao Lower Bound and the Fisher Information

The accuracy with which any parameter can be estimated from noisy data is limited by the amount of information on the parameter that is contained in the data. For any distribution of the noise affecting the input and the output, the lower bound to the covariance Σ that a parameter estimator can have is known as the *Cramér-Rao Lower Bound* (CRLB). The CLRB depends only on the statistical distribution of the noise and on the sensitivity of the data to the parameter. The inverse of the CRLB is known as the *Fisher Information* (FI), which indicates "how much information" on the parameter is contained in the data set. Technically, the FI is defined as

$$I(\theta) = \mathbf{E}\left(\frac{\partial}{\partial \theta} \log f(Y \mid \theta) \right)^2 \tag{11}$$

where $f(Y \mid \theta)$ is the probability density function of the observed data Y given the parameter θ. If the sensitivity of the likelihood of the noisy data to changes in the parameter is high, then the derivative in eq.11 is large and so is $I(\theta)$. In practice, the likelihood function $f(Y \mid \theta)$ is in general unknown so other quantities derived from the data are used. For example, if the data can be used to generate a vector X that is normally distributed having a mean that depends on the parameters, $\gamma(\theta)$, and a covariance Σ, the FI of the parameter θ contained in X can be obtained as

$$I(\theta) = \mathrm{J}_{\ }(\theta)^T \Sigma^{-1} \mathrm{J}_{\ }(\theta) \quad \text{where} \quad \mathrm{J}_{\ }(\theta) = \frac{\partial \gamma}{\partial \theta}. \tag{12}$$

Denoting Σ_λ as the covariance of the real and imaginary part of a pole, the FI of the frequency and the damping follows from eq.12 as

$$I(\xi, f) = \mathrm{J}_{\xi, f}^{\ T} \Sigma_\lambda^{-1} \mathrm{J}_{\ \xi, f} \tag{13}$$

where the sensitivity of the pole with respect to damping ratio and frequency is given by

$$\mathrm{J}_{\ \xi, f} = \frac{\partial(\Re(\lambda), \Im(\lambda))}{\partial(\xi, f)} = 2\pi \begin{bmatrix} -f & -\xi \\ -f\xi(1-\xi^2)^{-\frac{1}{2}} & \sqrt{1-\xi^2} \end{bmatrix}. \tag{14}$$

Due to the relation between the FI and the CRLB, an analytical relationship between the coefficients of variation of damping and frequency can be obtained from eq.14. This relation shows that the ratio depends only on the damping ratio. Assuming that the uncertainty region around the complex poles is circular, as depicted in the Monte-Carlo simulation in fig.1, the ratios between the coefficients of variation are shown in fig.4. As can be seen, the uncertainty on the damping ratios is around 50 times higher than that for the frequencies at $\xi = 0.02$, and the ratio is near 25 for $\xi = 0.05$.

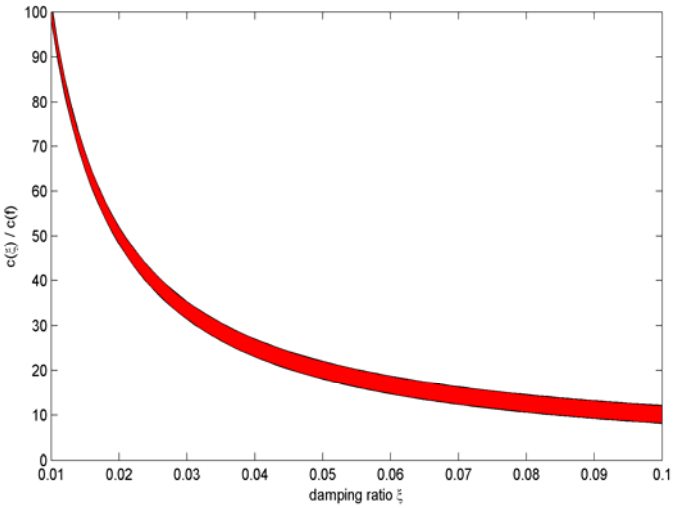

Figure 4. Range of the ratio of the coefficient of variation of damping and frequency when the uncertainty region around the pole is circular

Regression Analysis

Linear Regression

In a first step we considered fitting the damping values to a linear expression using a single regressor, x, namely

$$\zeta = \alpha_0 + \alpha_1 x \tag{15}$$

where x is taken as either: a) identified frequency (f), b) building height (H), c) spectral acceleration (SA), d) spectral velocity (SV), e) spectral displacement (SD), f) peak ground acceleration (PGA), g) peak ground velocity (PGV) or h) peak ground displacement (PGD) or their inverses. For each regression, the coefficient of determination was computed. This coefficient is defined as

$$R^2 = 1 - \frac{\sum_i (y_i - \bar{y})^2}{\sum_i (y_i - f_i)^2} \tag{16}$$

where y_i is the identified value, $\bar{y}$ is the mean of the identified results and f_i is the prediction given by the regression equation. The regression was carried out for the first mode damping ratio ζ_1 for steel, concrete, masonry, and wood buildings. When the mode considered is dominated by translation in one direction, the ground motion in this direction was used to compute the ground motion parameters. When the mode is strongly coupled, or torsional, we used the average of the ground motion parameters for the two directions. In the case of steel buildings the best correlation was found with building height and the results are depicted in fig.5. The results for concrete, masonry and wood, showing the correlation with height and the correlation that led to the highest R value are shown in fig.6 (a)-(f).

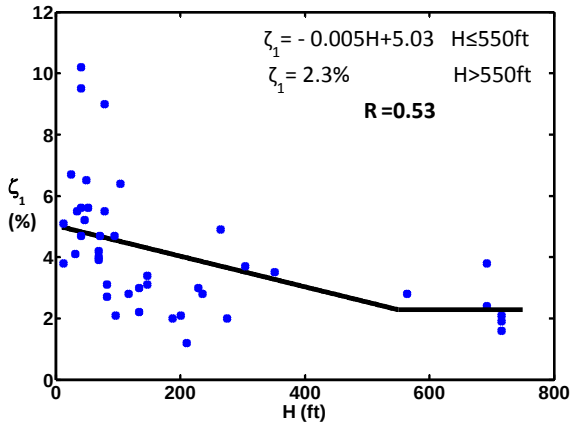

Figure 5. Linear regression for first mode damping ratio vs. building height - Steel buildings

Multivariate Regression

To investigate whether using more than one regressor could lead to major improvements, we looked at the use Artificial Neural Networks (ANN). The idea was not to propose an ANN to predict damping values but, if a simple network gave a notable improvement in the correlations, then it should be possible to extract the nonlinear relation of the network and a simplified expression perhaps could be formulated. To gain some appreciation of how the ANN performed and to gain some confidence in the extraction of the function, we first applied the methodology using a network having one input plus one hidden layer with two neurons. The results for concrete buildings is shown in fig.7, where the equation identified by the network proved to be

$$\zeta_1 = -0.37 \tanh\left(\frac{-3.7}{H} - 0.39\right) - 1.07 \tanh\left(\frac{-8.25}{H} - 9.09\right) - 1.04 \qquad (17)$$

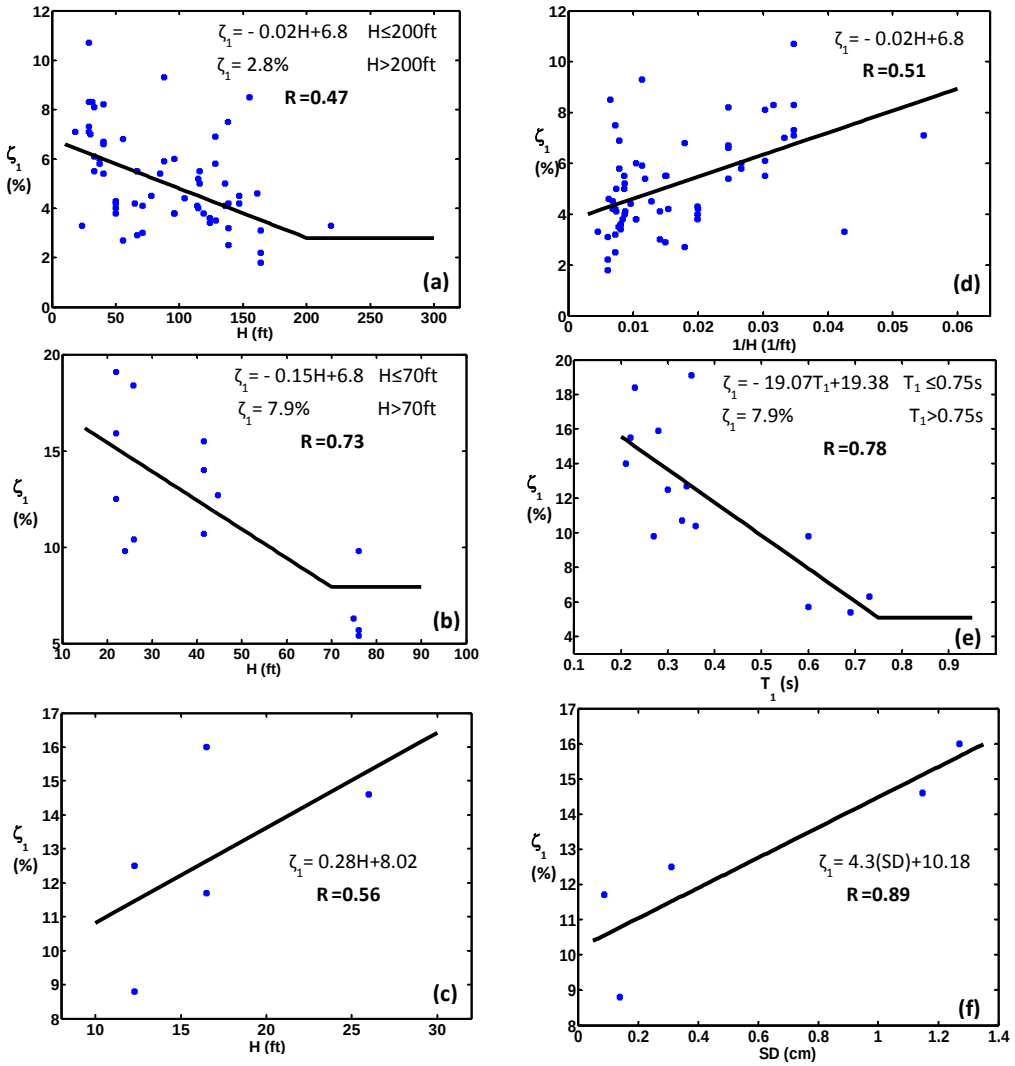

Figure 6. Linear regression for first mode damping ratio vs. building height and best linear regression for concrete (a) & (d), masonry (b) & (e), and wood (c) & (f) buildings respectively.

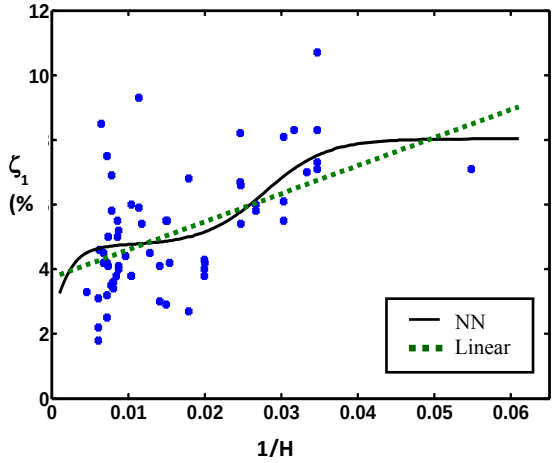

Figure 7. Non-linear regression using ANN for concrete buildings

Needless to say, there is no justification for recommending the complicated expression in eq.17, since the result is entirely dependent of the particular data set considered. Having established that the ANN was working properly we tried it with the same configuration but using two inputs. Table 2 shows the best R values obtained for each building type using one and two regressors as well as the linear regression result. In the two regressor case, the first regressor is either frequency or height or its reciprocal and the second regressor is any of the ground motion related parameters. Although the two-input ANN offered the highest R values, as expected, the improvements over the single input ANN are modest and it was concluded that there was no good reason to pursue it, given the available data.

Table 2. Summary of R values for the regression analysis

	R ANN 2 par	R ANN 1 par	R Linear
Steel	0.79	0.72	0.53
Concrete	0.68	0.64	0.51
Masonry	0.93	0.81	0.78

Conclusions

The analytical investigations show that damping ratios identified from earthquake records are realizations from a distribution with high variance. The reason for the high variance can be traced to the low sensitivity of the transient response to the damping but it can also be visualized from the pole location in the complex plane and the distribution of the uncertainty. In this regard the paper shows that the coefficient of variation of damping estimates are 25 to 50 times larger than the coefficient of variation of frequency estimates. The results of the present study are in agreement with previous results which indicate that the damping ratio increases with frequency. It is speculated here, however, that the causal relationship may be with the relative importance of dissipation through the soil-structure interface and not with frequency per se. The paper suggests that the relation between the damping of higher modes and the first one is likely governed by the efficiency with which the mode shape activates the dissipation mechanism. It was found that predictive equations more complex than linear regression with a single parameter could not be justified, given the data. All and all the results show that damping in steel buildings is larger than the 2% that is typically assigned while the widely used 5% is reasonable for concrete, if a single value is to be used.

Acknowledgements

The research reported in this paper was carried out with support from the California Strong Motion Instrumentation Program (CSMIP) through standard agreement 1010-934. This support is gratefully acknowledged.

Appendix A – Identification

Time domain algorithms are typically based on an indirect approach. Namely, a model mapping the sampled input and the sampled output is obtained and then it is converted to continuous time. The postulated model in sampled time has the form

$$x(k+1) = A_d x(k) + B_d \ddot{x}_g(k) \tag{a.1}$$

where the measurements are given by

$$\ddot{y}(k) = Cx(k) \tag{a.2}$$

The procedure begins by noting that for the model in eq.a.1 the output is related to the input as

$$y(k) = \sum_{j=1}^{k} Y_j \ddot{x}_g(k-j) \tag{a.3}$$

where Y_j, known as a Markov Parameter (MP) is given by

$$Y_j = CA_d^{j-1}B_d \tag{a.4}$$

Once the MP are obtained from eq.a.3, the next task is to untangle the matrices $\{A_d, B_d, C\}$ from the triple product. This is done by defining the Hankel matrix H_k as

$$H_k = \begin{bmatrix} Y_{k+1} & Y_{k+2} & \cdots & Y_{k+\beta} \\ Y_{k+2} & Y_{k+3} & \cdots & Y_{k+\beta} \\ \vdots & \vdots & \vdots & \vdots \\ Y_{k+\alpha} & . & \cdots & Y_{k+\beta+\alpha-1} \end{bmatrix} \tag{a.5}$$

where α and β are user defined parameters and noting that with

$$P_\alpha = \begin{bmatrix} C_d \\ C_d A_d \\ \vdots \\ C_d A_d^{\alpha-1} \end{bmatrix} \tag{a.6}$$

and

$$Q_\beta = [B_d \quad A_d B_d \quad A_d^2 B_d \quad \cdots \quad A_d^{\beta-1} B_d] \tag{a.7}$$

$$H_k = P_\alpha A_d^k Q_\beta \tag{a.8}$$

so it follows that H_0

$$H_0 = P_\alpha Q_\beta \tag{a.9}$$

one then performs a singular value decomposition of H_0, namely

$$H_0 = R \Sigma S^T \tag{a.10}$$

and after retaining only the N most important singular values, has

$$H_0 = R_N \Sigma_N S_N{}^T \tag{a.11}$$

where R_N contains the first N columns of R, S_N the first N columns of S and Σ_N is the diagonal matrix having the N significant singular values. Splitting the diagonal singular value matrix into the product of two matrices (E_1 and E_2)

$$E_1 E_2 = \Sigma_N \tag{a.12}$$

gives

$$H_0 = (R_N E_1)(E_2 S_N^T) \tag{a.13}$$

and one can then take

$$P_\alpha = R_N E_1 \tag{a.14}$$

$$Q_\beta = E_2 S_N^T \tag{a.15}$$

from where, given the definitions in eq.'s a.6 and a.7 one has that

- The first *m* rows of P_α provide a realization for C.
- The first *r* columns of Q_β provide a realization for B_d.

The matrix A_d can be obtained from the block Hankel matrix for k = 1, namely, given that

$$H_1 = P_\alpha A_d Q_\beta = R_N E_1 A_d E_2 S_N^T \tag{a.16}$$

and the fact that R_N and S_N are orthonormal one gets

$$A_d = E_1^{-1} R_N^T H_1 S_N E_2^{-1} \tag{a.17}$$

Discrete to Continuous Transfer

Once the sampled time model is available its conversion to continuous time follows as (Bernal 2006)

$$A_c = \frac{1}{\Delta t} \ln(A_d) \tag{a.18}$$

$$B_c = \frac{1}{\Delta t} A_d^{-1} B_d \tag{a.19}$$

$$C_c = C \tag{a.20}$$

The damping ratios are obtained as the real part of the eigenvalues of A_c divided by their magnitude.

Appendix B - Data

Table B.1. Data for regression analysis

Station #	Earthquake	ζ_1(%)	T_1(s)	H(ft)	SA(g)	SV(cm/s)	SD(cm)	PGA(g)	PGV(cm/s)	PGD(cm)
58262	Loma Prieta	3.3	0.27	23.5	0.195	8.33	0.362	0.108	12.77	2.38
47391	Morgan Hill 84	7	0.59	30	0.129	11.87	1.111	0.066	6.52	3.05
57502	LomaPrieta	8.3	0.23	31.6	0.299	10.95	0.409	0.109	27.96	19.67
58334	Loma Prieta	6.4	0.20	*NA**	0.161	5.05	0.161	0.075	8.29	1.40
58334	Berkeley 71667366	5.5	0.18	*NA*	0.133	3.78	0.109	0.040	1.17	0.06
58334	Piedmont	4.9	0.18	*NA*	0.135	3.80	0.109	0.068	2.75	0.22
58348	Loma Prieta	8.2	0.45	40.6	0.222	15.60	1.119	0.117	19.98	5.85
58348	Lafayette	6.7	0.42	40.6	0.063	4.11	0.272	0.055	2.12	0.17
23511	Whittier	5.4	0.29	40.5	0.110	4.89	0.222	0.046	2.04	0.14
23511	Chinohills	6.6	0.34	40.5	0.232	12.17	0.650	0.130	11.94	2.30
23495	Big Bear	7.3	0.52	28.8	0.369	29.72	2.438	0.174	12.40	1.92
23495	Landers	10.7	0.45	28.8	0.272	19.14	1.372	0.105	11.29	3.21
23495	Palm Springs	7.1	0.40	28.8	0.137	8.54	0.544	0.042	3.62	0.55
23495	SanBernardino	8.3	0.43	28.8	0.048	3.25	0.225	0.059	2.30	0.16
58263	Loma Prieta	4	0.15	*NA*	0.139	3.17	0.074	0.071	10.85	4.39
58503	Loma Prieta	6	0.29	37.5	0.204	9.17	0.419	0.102	14.51	2.25
58503	Elcerrito	5.8	0.25	37.5	0.103	4.06	0.164	0.059	2.01	0.09
23622	Landers	7.1	0.24	18.25	0.164	6.16	0.235	0.090	14.40	8.09
25213	Santa Barbara	5.5	0.32	33	1.043	52.15	2.660	0.378	34.26	5.47
58235	Morgan Hill 84	6.1	0.25	33	0.201	7.73	0.302	0.060	4.23	0.89
58235	Loma Prieta	8.1	0.30	33	0.728	33.71	1.592	0.315	36.57	7.34
58196	Lafayette	6.8	0.33	55.8	0.115	6.01	0.319	0.056	2.40	0.13
58196	Piedmont	2.7	0.33	55.8	0.128	6.66	0.353	0.061	2.42	0.23
89770	Ferndale 2007	4.1	0.37	*NA*	0.664	38.69	2.298	0.231	21.29	4.86
58488	Loma Prieta	4.2	0.25	50	0.136	5.31	0.211	0.052	4.21	0.85
58462	Loma Prieta	5.4	0.96	84.8	0.106	15.86	2.427	0.103	10.41	2.01
14311	Whittier	3	0.34	71	0.243	12.90	0.699	0.094	6.15	0.72
14311	Chinohills	4.1	0.32	71	0.087	4.38	0.225	0.066	7.66	1.43
24463	Whittier	3.8	1.43	119	0.091	20.24	4.602	0.131	12.73	1.95
12284	Borrego Springs Jul2010	4.3	0.68	50.2	0.044	4.67	0.503	0.053	2.18	0.31
12284	Calexico Apr2010	4	0.69	50.2	0.104	11.22	1.231	0.052	4.29	3.16
12284	Palm Springs	3.8	0.60	50.2	0.082	7.71	0.739	0.090	8.06	2.40
23285	San Bernardino	2.9	0.52	67	0.012	1.01	0.084	0.059	1.35	0.07
24468	Northridge	4	1.59	114.8	0.082	20.29	5.126	0.117	8.69	1.42
24468	Whittier	5.2	1.54	114.8	0.113	27.05	6.624	0.324	20.07	2.37
24579	Landers	5.8	1.43	128	0.053	11.80	2.683	0.038	6.76	4.15
24579	Northridge	6.9	1.52	128	0.092	21.67	5.225	0.150	13.43	2.90

Station #	Earthquake	ζ_1(%)	T_1(s)	H(ft)	SA(g)	SV(cm/s)	SD(cm)	PGA(g)	PGV(cm/s)	PGD(cm)
47459	Loma Prieta	5.5	0.35	66.3	0.953	52.58	2.957	0.359	54.87	18.23
58479	Loma Prieta	4.2	0.34	65	0.164	8.65	0.465	0.070	15.10	4.21
58490	Loma Prieta	4.5	1.00	78	0.216	33.63	5.353	0.114	16.16	2.66
24655	Northridge	5.5	0.52	67	0.441	35.48	2.911	0.286	19.08	4.44
24571	Landers	4.1	2.00	136	0.044	13.80	4.392	0.036	6.37	2.03
24571	Northridge	4.1	2.13	136	0.024	8.08	2.736	0.156	8.92	1.28
24571	Sierra Madre	5	1.96	136	0.030	9.03	2.819	0.104	7.54	0.75
58394	Loma Prieta	4.4	1.72	104	0.136	36.50	10.017	0.125	14.95	3.31
24385	Sierra Madre	5.9	0.54	88	0.103	8.66	0.741	0.074	4.62	0.67
24385	Whittier	9.3	0.55	88	0.241	20.67	1.807	0.209	10.97	1.00
57355	Morgan Hill 84	3.6	0.91	124	0.144	20.48	2.963	0.058	12.28	3.38
57355	Alum Rock	3.4	1.04	124	0.063	10.26	1.700	0.071	5.81	1.14
57355	Loma Prieta	3.6	1.01	124	0.133	20.92	3.363	0.086	18.11	9.93
57356	Morgan Hill 84	3.8	0.61	96	0.139	13.17	1.270	0.054	12.10	2.84
57356	Loma Prieta	6	0.67	96	0.185	19.40	2.072	0.093	16.55	7.26
57356	Alum Rock	3.8	0.73	96	0.088	10.05	1.167	0.114	7.98	1.12
24322	Northridge	1.8	3.13	164	0.064	31.41	15.622	0.832	60.65	13.55
24322	Whittier	3.1	2.50	164	0.008	3.31	1.315	0.257	8.11	0.49
24322	Chinohills	2.2	1.54	164	0.015	3.66	0.896	0.073	3.39	0.29
58364	Loma Prieta	3.5	0.80	128.5	0.103	12.92	1.645	0.047	7.57	1.35
14578	Chinohills	5.5	1.25	116	0.050	9.73	1.936	0.100	9.11	1.04
14578	Northridge	5	1.19	116	0.034	6.29	1.192	0.069	5.47	1.36
24601	Northridge	4.2	1.16	138.7	0.029	5.24	0.970	0.021	1.66	0.58
24601	Sierra Madre	2.5	1.01	138.7	0.068	10.67	1.715	0.068	5.24	0.71
24601	Landers	3.2	1.06	138.7	0.102	16.94	2.868	0.043	7.29	6.53
24581	Chinohills	8.5	1.79	155	0.010	2.68	0.763	0.059	4.09	0.35
24236	Whittier	7.5	1.85	138.3	0.041	11.98	3.532	0.118	9.46	1.37
58483	Loma Prieta	3.3	2.44	219	0.057	21.67	8.414	0.123	17.09	4.31
13589	Landers	4.5	0.82	146.9	0.124	15.86	2.069	0.041	6.31	2.84
13589	Northridge	4.2	0.85	146.9	0.092	12.16	1.640	0.076	5.56	1.74
58639	Piedmont	4.1	0.81	114	0.012	1.52	0.195	0.031	1.55	0.11
24680	Chinohills	4.6	1.47	161	0.011	2.62	0.613	0.027	2.01	0.25
58496	Loma Prieta	6.7	0.33	25.2	0.228	11.67	0.609	0.102	6.41	0.919
24198	Chinohills	5.5	0.68	34	0.077	8.28	0.903	0.074	5.76	0.628
01699	Calexico May2010	5.1	0.16	12.4	0.149	3.62	0.090	0.059	2.54	0.216
01699	Ocotillo Jun2010	3.8	0.15	12.4	0.142	3.39	0.082	0.062	3.95	1.351
54331	Mammoth Lakes	4.1	0.17	31.9	0.171	4.59	0.126	0.124	3.85	0.215

Station #	Earthquake	ζ_1(%)	T_1(s)	H(ft)	SA(g)	SV(cm/s)	SD(cm)	PGA(g)	PGV(cm/s)	PGD(cm)
58506	Loma Prieta	5.2	0.71	46.2	0.282	31.22	3.524	0.110	20.35	4.730
23516	Landers	10.2	0.56	41.3	0.205	17.74	1.568	0.082	15.07	7.640
23516	Chinohills	9.5	0.49	41.3	0.161	12.28	0.958	0.069	4.78	0.419
23516	San Bernardino	4.7	0.56	41.3	0.125	10.85	0.959	0.102	7.30	0.467
57562	Loma Prieta	6.5	0.74	49.5	0.320	36.72	4.297	0.177	18.47	6.665
24104	Chatsworth	5.6	0.46	41	0.161	11.64	0.858	0.084	6.12	0.365
24370	Whittier	2.7	1.28	82.5	0.088	17.66	3.604	0.226	12.51	1.270
24370	Sierra Madre	3.1	1.28	82.5	0.052	10.38	2.118	0.124	5.84	0.782
24609	Landers	9	0.74	78.5	0.153	17.57	2.057	0.083	10.40	5.070
24609	Northridge	5.5	0.75	78.5	0.083	9.75	1.167	0.056	9.29	2.720
14323	Whittier	6.4	1.39	104	0.035	7.63	1.688	0.073	8.53	1.163
24652	Northridge	4.7	0.26	71.5	0.344	13.89	0.573	0.205	14.04	3.069
23481	Landers	4.7	1.59	94.4	0.038	9.29	2.347	0.059	5.86	2.279
23515	Landers	2.8	2.00	117.6	0.091	28.47	9.063	0.088	14.95	7.451
23634	BigBear	4.2	0.50	69	0.104	8.01	0.631	0.062	5.04	1.471
23634	Landers	3.9	0.49	69	0.175	13.45	1.055	0.080	12.35	6.510
23634	Northridge	4	0.49	69	0.103	7.87	0.611	0.049	4.28	0.724
24248	Chinohills	3.1	0.69	147	0.048	5.19	0.569	0.052	3.16	0.521
24248	Whittier Narrows	3.4	0.65	147	0.010	0.98	0.101	0.051	1.27	0.064
24249	Chinohills	3	0.71	134	0.065	7.16	0.808	0.059	2.91	0.326
24249	Whittier Narrows	2.2	0.68	134	0.010	1.05	0.113	0.045	1.31	0.070
24514	Whittier	2.1	0.34	96	0.184	9.89	0.541	0.057	3.68	0.561
58261	Loma Prieta	5.6	0.69	52.5	0.229	24.62	2.702	0.061	8.61	1.938
14533	Whittier	4.9	1.19	265	0.067	12.48	2.365	0.048	5.73	1.244
14654	Northridge	2	2.08	188	0.046	15.10	5.007	0.128	11.39	3.149
24288	Chinohills	3.5	1.16	351.2	0.045	8.25	1.527	0.067	6.47	1.021
24569	Northridge	2.8	1.18	236	0.119	21.86	4.092	0.137	12.56	3.104
24602	Chinohills	1.9	1.79	716	0.013	3.67	1.044	0.078	6.59	0.925
24602	Landers	2.1	5.88	716	0.017	15.94	14.927	0.121	7.73	4.005
24602	Northridge	1.6	1.85	716	0.071	20.39	6.009	0.159	12.71	2.955
24602	Sierra Madre	1.6	1.72	716	0.027	7.38	2.026	0.113	8.05	0.935
24629	Chinohills	3.8	1.92	692.5	0.010	3.07	0.939	0.065	4.97	0.642
24629	Northridge	2.4	1.85	692.5	0.060	17.38	5.124	0.099	8.42	3.061
24643	Northridge	3.7	0.82	304	0.443	56.66	7.392	0.260	16.18	4.880
57318	Alum Rock	2	2.17	275	0.020	6.95	2.404	0.063	6.09	1.184
57357	Loma Prieta	1.2	2.22	210.6	0.218	75.58	26.730	0.090	21.23	8.584
58354	Loma Prieta	2.1	1.33	201	0.039	8.12	1.724	0.079	6.85	0.795

Station #	Earthquake	ζ_1(%)	T_1(s)	H(ft)	SA(g)	SV(cm/s)	SD(cm)	PGA(g)	PGV(cm/s)	PGD(cm)
58480	Loma Prieta	3	2.27	229.3	0.034	11.94	4.317	0.161	15.81	2.649
58532	Loma Prieta	2.8	2.17	564	0.159	54.07	18.709	0.203	26.39	7.879
12266	Anza	18.4	0.05	25.8	0.197	1.67	0.014	0.0750	2.510	0.148
14606	Northridge	5.4	0.19	76	0.093	2.70	0.079	0.1100	8.626	1.571
14606	Chinohills	9.8	0.10	76	0.263	4.19	0.068	0.1290	11.922	1.824
14606	Whittier Narrows	5.7	0.18	76	0.023	0.63	0.018	0.2196	6.053	0.221
24517	Landers	10.7	0.09	41.5	0.139	2.03	0.030	0.0536	7.119	3.158
24517	Northridge	15.5	0.06	41.5	0.119	1.20	0.012	0.0555	9.274	2.530
24517	Whittier	14	0.07	41.5	0.133	1.48	0.017	0.0510	2.806	0.176
57476	Loma Prieta	10.4	0.10	26	0.630	9.46	0.145	0.2647	3.599	0.189
58264	Loma Prieta	9.8	0.10	24	0.477	7.60	0.123	0.2081	33.690	14.157
58492	Loma Prieta	6.3	0.16	74.9	0.195	4.82	0.122	0.0582	7.827	2.118
89473	Petrolia	19.1	0.05	22	0.216	1.77	0.015	0.1263	17.767	4.415
89473	Ferndale Jan2010	12.5	0.08	22	0.366	4.57	0.058	0.1414	11.807	2.137
89473	Petrolia Aftershock	15.9	0.06	22	0.482	4.74	0.047	0.1599	12.489	2.330
89494	Ferndale Jan2010	12.7	0.08	44.7	0.565	6.94	0.087	0.2161	22.426	5.183
12759	Anza	12.5	0.08	12.3	0.4334	5.41	0.069	0.2247	10.858	0.923
12759	Borrego Springs Jul2010	8.8	0.11	12.3	0.1933	3.43	0.062	0.0657	4.441	0.785
36695	San Simeon	16	0.06	16.5	1.2786	12.47	0.124	0.4484	30.092	7.341
36695	Atascadero	11.7	0.09	16.5	0.1095	1.46	0.020	0.0562	1.426	0.049
89687	Ferndale Jan2010	14.6	0.07	26	0.5131	5.48	0.060	0.2462	26.074	5.340

**NA*: Information is not available on CSMIP website

References

Bernal, D. (2007) Optimal Discrete to Continuous Transfer for Band Limited Inputs. *Journal of Engineering Mechanics,* 133(12), 1370-1377.

Gersch, W. (1974). On the achievable accuracy of structural system parameter estimates, *Journal of Sound and Vibration*, 34(1) 63–79.

Hart, G.C. & Vasudevan R. (1975) Earthquake design of buildings: damping. *Journal of the Structural Division, ASCE 1975;*101(1):11–29.

Heylen, W., Lammens, S. & Sas, P. (1997) Modal Analysis Theory and Testing. *KUL Press, Leuven.*

Jeary, A. P. (1986). Damping in tall buildings—A mechanism and a predictor. *Earthquake Eng. Struct. Dyn.,* 14, 733–750.

Juang, J. (1994) Applied system identification. *Englewood Cliffs, NJ: PTR Prentice Hall, Inc , 1994.*

Lagomarsino, S. (1993). Forecast models for damping and vibration periods of buildings. *J. Wind. Eng. Ind. Aerodyn.,* 48, 221–239.

McVerry, G.H. (1979). Frequency Domain Identification of Structural Models from Earthquake Records. *Ph.D. thesis, California Institute of Technology.*

McVerry, G.H. (1980) Structural identification in the frequency domain from earthquake records. *Earthquake Engineering and Structural Dynamics,* 8:161–80.

Sasaki, A., Suganuma, S., Suda, K. & Tamura, Y. (1998). ‘‘Full-scale database on dynamic properties of buildings—Frequency and amplitude dependencies of buildings.’’ *Proc., Annual Meeting of the Architectural Institute of Japan (AIJ), Fukuoka, AIJ Japan, B-2,* 379–380.

Tamura, Y. & Suganuma, S. (1996). Evaluation of amplitude dependent damping and natural frequency of buildings during strong winds. *J. Wind. Eng. Ind. Aerodyn.*, 59, 115–130.

Van Overschee, P., & De Moor, B. (1996) Subspace identification for linear systems: Theory, implementation, applications. *Kluwer Academic, Boston.*

Verhaegen & Verdult (2007) Filtering and system identification: An introduction. *Cambridge University Press.*

Zhang, Z. & Cho, C. (2009) Experimental Study on Damping Ratios of in-situ Buildings. *World Academy of Science, Engineering and Technology,* 26, 614-618.